J. Am. Chem. Soc. 1986, 108, 601-606 601

Theoretical Studies of Substituent Effects on the Additions of Amines to Carbonyl Compounds: A Relation among Energetics, Structures, and Isotope Effects

Hiroshi Yamataka,*[1a] Shigeru Nagase,*[1b] Takashi Ando,[1c] and Terukiyo Hanafusa[1a]

Contribution from the Institute of Scientific and Industrial Research, Osaka University, Ibaraki, Osaka 567, Japan, Department of Chemistry, Faculty of Education, Yokohama National University, Hodogaya, Yokohama 240, Japan, and Department of Chemistry, Shiga University of Medical Science, Otsu, Shiga 520-21, Japan. *Received January 21, 1985*

Abstract: Addition reactions of amines (NH_3, CH_3NH_2, and NHF_2) to carbonyl compounds (CH_2O, CH_3CHO, and CF_2O) were investigated by using an ab initio molecular orbital method with the object of gaining an insight to a relation between transition-state structures and reactivities. Structures of reactants, transition states, and products were fully optimized with the 3-21G basis set. Kinetic and equilibrium isotope effects were determined by Bigeleisen's equation from the calculated vibrational frequencies. Single-point energy calculations were carried out for all the structures with the 6-31G* basis set. It was found that the reaction of NHF_2 with CH_2O exhibits different behavior from other reactions, NH_3–CH_2O, CH_3NH_2–CH_2O, NH_3–CH_3CHO, NH_3–CF_2O, and NH_3–HOCHO which form a family of reactions. Within the family, activation energy becomes smaller for a more exothermic reaction; thus the Bell–Evans–Polanyi–Leffler–Hammond rule holds. In contrast, the transition-state structures and the kinetic isotope effects are nearly the same for these reactions in spite of a large variation in reactivity (17 kcal/mol between NH_3–CF_2O and NH_3–HOCHO, corresponding to the rate ratio of 10^{12}), which is a breakdown of the above rule. The differences in the structures of the transition states between the family of reactions and the NHF_2–CH_2O reaction are consistent with the prediction based on the More O'Ferrall–Jencks diagram. The variations in the kinetic isotope effects are also consistent with the differences in the transition-state structures; this supports the assumption that the magnitude of a kinetic isotope effect is a measure of a transition-state structure.

It is a long-standing goal of physical organic chemistry to establish the method of predicting a variation in the structures and properties of the transition states of chemical reactions. There are a number of theories presented for this purpose.[2–7] These theories deal with the variation in the barrier height and/or the position of the barrier along the reaction coordinate caused by a change in the reaction energy. Although the method of derivation is different, these theories are similar in a qualitative prediction that for a more exothermic reaction the barrier height becomes lower and the position of the barrier tends to be earlier along the reaction coordinate. In fact, it was recently shown that the equations derived from these theories are specific cases of a general expression.[8]

It should be noted here that the barrier height is concerned with energy while the position of the barrier relates to the structure of the transition state. Thus, it is often necessary to consider these two properties separately. A few analytical methods have been presented in order to estimate the variation in the structure of the transition state, such as Thornton's rule[9] and the More O'Ferrall–Jencks energy diagram procedure.[10,11] The latter method is especially useful because its operation procedure is rather simple and it can be applied to many types of reactions.

However, it is often very difficult to test these theories experimentally. Although there are a few reactions in which both activation and reaction energies have been measured,[12,13] reliable experimental techniques to detect a variation in a transition-state structure are limited, and therefore it is not easy to examine the relation among energetics and transition-state structures. A kinetic isotope effect is believed to be the most direct and sensitive probe of the structural variation of a transition state;[14] certainly the magnitudes of kinetic isotope effects are directly related to the variation of force field, but there is no strong evidence in support of the assumption that the variation of force field is related to the variation of the structure of the transition state in the expected manner.

In the present investigation, ab initio MO calculations were carried out for addition reactions of amines with carbonyl compounds. This reaction system was chosen because the reaction was expected to proceed via a single step and substituent effects both on nucleophile and electrophile could be investigated. Since the MO method provides information concerning the effect of substituents on activation and reaction energies, on a transition-state structure, and on kinetic and equilibrium isotope effects at the same time and also because it is free from solvent effect, MO calculations provide a convenient method for testing certain predictions of the aforementioned theories.

Calculations and Results

Ab initio MO calculations were carried out[15,16] for the five combinations of amines and carbonyl compounds: NH_3–CF_2O (reaction 1), CH_3NH_2–CH_2O (2), NH_3–CH_2O (3), NH_3–CH_3CHO (4), and NHF_2–CH_2O (6). Calculations on the NH_3–HOCHO system (reaction 5) has been reported in the lit-

---

(1) (a) Osaka University. (b) Yokohama National University. (c) Shiga University of Medical Science.

(2) Leffler, J. E. *Science (Washington, D.C.)* **1953**, *117*, 340–341.

(3) Hammond, G. S. *J. Am. Chem. Soc.* **1955**, *77*, 334–338.

(4) (a) Bell, R. P. *Proc. R. Soc. London, A* **1936**, *154*, 414–429. (b) Evans, M. G.; Polanyi, M. *Trans. Faraday Soc.* **1936**, *32*, 1333–1360. (c) Evans, M. G.; Polanyi, M. *Ibid.* **1938**, *34*, 11–29.

(5) Johnston, H. S. "Gas Phase Reaction Rate Theory"; Ronald Press: New York, 1966.

(6) (a) Miller, A. R. *J. Am. Chem. Soc.* **1978**, *100*, 1984–1992. (b) Murdoch, J. R. *Ibid.* **1983**, *105*, 2667–2672. (c) Lewis, E. S.; Shen, C. C.; More O'Ferrall, R. A. *J. Chem. Soc., Perkin Trans. 2* **1981**, 1084–1088.

(7) (a) Marcus, R. A. *J. Phys. Chem.* **1968**, *72*, 891–899. (b) Cohen, A. O.; Marcus, R. A. *Ibid.* **1968**, *72*, 4249–4256.

(8) Murdoch, J. R. *J. Am. Chem. Soc.* **1983**, *105*, 2159–2164.

(9) Thornton, E. R. *J. Am. Chem. Soc.* **1967**, *89*, 2915–2927.

(10) More O'Ferrall, R. A. *J. Chem. Soc. B* **1970**, 274–277.

(11) Jencks, W. P. *Chem. Rev.* **1972**, *72*, 705–718.

(12) (a) Lewis, E. S.; Kukes, S.; Slater, C. D. *J. Am. Chem. Soc.* **1980**, *102*, 1619–1623. (b) Pellerite, M. J.; Brauman, J. I. *Ibid.* **1980**, *102*, 5993–5999. (c) Gajewski, J. J. *Ibid.* **1979**, *101*, 4393–4394. (d) Albery, J. A.; Kreevoy, M. M. In "Advances in Physical Organic Chemistry"; Gold, V., Bethell, D., Eds.; Academic Press: London, 1978; Vol. 16.

(13) (a) Magnoli, D. E.; Murdoch, J. R. *J. Am. Chem. Soc.* **1981**, *103*, 7465–7469. (b) Murdoch, J. R.; Bryson, J. A.; McMillen, D. F.; Brauman, J. I. *Ibid.* **1982**, *104*, 600–610. (c) Murdoch, J. R. *Ibid.* **1983**, *105*, 2660–2667.

(14) Melander, L.; Saunders, W. H., Jr. "Reaction Rates of Isotopic Molecules"; Wiley-Interscience : New York, 1980.

(15) An IMSPACK program: Morokuma, K.; Kato, S.; Kitaura, K.; Ohmine, I.; Sakai, S.; Obara, S. IMS Computer Library Program, No. 0372, 1982.

(16) GAUSSIAN 80 Program: Binkley, J. S.; Whiteside, R. A.; Krishnan, R.; Seager, R.; DeFrees, D. J.; Schlegel, H. B.; Kaln, L. R.; Pople, J. A. *QCPE* **1981**, *13*, 406.

0002-7863/86/1508-0601$01.50/0

Table I. 3-21G Optimized Structures of Reactants, Transition States, and Products for Addition Reactions of Amines to Carbonyl Compounds[a]

species	coordinates	parameters	species	coordinates	parameters
NH_3	N_1H_2	1.003	NHF_2–CH_2O	C_1O_2	1.304
	$X_3H_2N_1$	1.0: 90.0	TS	$N_3C_1O_2$	1.959; 83.6
	$H_{4,5}N_1H_2H_3$	1.003; 112.4; ±116.1		$H_4N_3C_1O_2$	1.315; 64.8; 0.0
NHF_2	N_1H_2	1.013		$H_{5,6}C_1O_2N_3$	1.075; 120.9; ±98.5
	$X_3N_1H_2$	1.0; 90.0		$F_{7,8}N_3C_1O_2$	1.416; 122.9; ±110.3
	$F_{4,5}N_1H_2X_3$	1.422; 101.3; ± 127.2	NH_3–CF_2O	C_1O_2	1.305
CH_3NH_2	C_1N_2	1.471	TS	$N_3C_1O_2$	1.557; 96.7
	$H_3C_1N_2$	1.090; 114.8		$H_4N_3C_1O_2$	1.247; 73.0; 0.0
	$H_{4,5}C_1N_2H_3$	1.083; 109.0; ±121.5		$F_{5,6}C_1O_2N_3$	1.357; 118.3; ±114.8
	$H_{6,7}N_2C_1H_3$	1.004; 113.6; ± 64.2		$H_{7,8}N_3C_1O_2$	1.010; 114.6; ±114.3
CH_2O	C_1O_2	1.207	NH_3–CH_2O	C_1O_2	1.441
	$H_3C_1O_2$	1.083; 122.5	prod	$N_3C_1O_2$	1.438; 115.9
	$H_4C_1O_2H_3$	1.083; 122.5; 180.0		$H_4O_2C_1N_3$	0.967; 110.6; 62.9
CH_3CHO	C_1O_2	1.208		$H_5C_1O_2N_3$	1.076; 104.2; 120.0
	$H_3C_1O_2$	1.087; 120.9		$H_6C_1O_2N_3$	1.082; 110.4; 123.3
	$C_4C_1O_2H_3$	1.507; 124.8; 180.0		$H_7N_3C_1O_2$	1.002; 104.9; 116.5
	$H_5C_4C_1H_3$	1.080; 109.9; 180.0		$H_8N_3C_1O_2$	1.002; 97.2; 127.3
	$H_{6,7}C_4C_1H_3$	1.086; 109.9; ±59.1	CH_3NH_2–CH_2O	C_1O_2	1.429
CF_2O	C_1O_2	1.169	prod	$N_3C_1O_2$	1.451; 110.3
	$F_3C_1O_2$	1.322; 125.8		$H_4O_2C_1N_3$	0.968; 108.3; 47.2
	$F_4C_1O_2F_3$	1.322; 125.8; 180.0		$H_5C_1O_2N_3$	1.084; 105.1; 123.5
HOCHO	O_2C_1	1.198		$H_6C_1O_2N_3$	1.085; 111.6; −119.3
	$H_3C_1O_2$	1.074; 125.8		$H_7N_3C_1O_2$	1.004; 112.7; 62.3
	$O_4C_1O_2H_3$	1.350; 124.7; 179.9		$C_8N_3C_1O_2$	1.465; 116.8; 196.8
	$H_5O_4C_1O_2$	0.970; 112.7; 0.0		$H_9C_8N_3C_1$	1.082; 109.2; 174.5
NH_3–CH_2O	C_1O_2	1.371		$H_{10}C_8N_3C_1$	1.083; 109.1; 56.7
TS	$N_3C_1O_2$	1.624; 94.2		$H_{11}C_8N_3C_1$	1.090; 114.0; −64.2
	$H_{4,5}C_1O_2N_3$	1.084; 118.7; ±110.7	NH_3–CH_3CHO	C_1O_2	1.435
	$H_6O_2C_1N_3$	1.416; 76.3; 0.0	prod	$N_3C_1O_2$	1.452; 109.8
	$H_{7,8}N_3C_1O_2$	1.009; 116.5; ±112.5		$H_4O_2C_1N_3$	0.967; 108.2; 39.3
CH_3NH_2–CH_2O	C_1O_2	1.377		$C_5C_1O_2N_3$	1.526; 105.4; 123.7
TS	$N_3C_1O_2$	1.603; 94.5		$H_6C_1O_2N_3$	1.083; 110.5; −117.6
	$H_4N_3C_1O_2$	1.180; 74.2; 2.1		$H_7N_3C_1O_2$	1.003; 115.2; 76.1
	$H_5C_1O_2N_3$	1.085; 118.4; 111.4		$H_8N_3C_1O_2$	1.000; 116.2; −147.7
	$H_6C_1O_2N_3$	1.085; 118.4; −111.5		$H_9C_5C_1O_2$	1.082; 110.2; 57.7
	$H_7N_3C_1O_2$	1.009; 114.8; 113.8		$H_{10}C_5C_1O_2$	1.083; 109.0; −60.9
	$C_8N_3C_1O_2$	1.486; 117.3; −109.9		$H_{11}C_5C_1O_2$	1.083; 110.5; 178.8
	$H_9C_8N_3C_1$	1.081; 109.9; 166.0	NHF_2–CH_2O	C_1O_2	1.401
	$H_{10}C_8N_3C_1$	1.080; 107.7; 47.0	prod	$N_3C_1O_2$	1.495; 109.8
	$H_{11}C_8N_3C_1$	1.081; 110.8; −72.8		$H_4O_2C_1N_3$	0.967; 112.1; 66.3
NH_3–CH_3CHO	C_1O_2	1.373		$H_5C_1O_2N_3$	1.072; 108.5; 118.0
TS	$N_3C_1O_2$	1.630; 93.7		$H_6C_1O_2N_3$	1.078; 114.4; 117.1
	$H_4N_3C_1O_2$	1.181; 73.6; 1.3		$F_7N_3C_1O_2$	1.419; 103.9; 73.8
	$C_5C_1O_2N_3$	1.520; 116.7; 113.2		$F_8N_3C_1O_2$	1.425; 101.5; 180.8
	$H_6C_5O_2N_3$	1.085; 117.9; −109.3	NH_3–CF_2O	C_1O_2	1.368
	$H_7N_3C_1O_2$	1.009; 116.7; 115.1	prod	$N_3C_1O_2$	1.395; 112.3
	$H_8N_3C_1O_2$	1.009; 116.1; −110.3		$H_4O_2C_1N_3$	0.966; 111.5; 50.6
	$H_9C_5C_1O_2$	1.083; 108.3; 70.4		$F_5C_1O_2N_3$	1.361; 105.7; 125.2
	$H_{10}C_5C_1O_2$	1.083; 109.1; −46.5		$F_6C_1O_2N_3$	1.365; 111.4; 120.8
	$H_{11}C_5C_1O_2$	1.084; 112.5; −169.2		$H_7N_3O_2C_1$	0.999; 147.6; 30.8
				$H_8N_3O_2C_1$	0.999; 94.9; 132.8

[a] PQRS *l*;*m*;*n* indicates that bond length P–Q is *l* Å, bond angle P–Q–R is *m* degree, and dihedral angle P–Q–R–S is *n* degree. X in coordinates refers to a dummy atom. TS and prod are transition state and product species, respectively.

Table II. Charge Densities and HOMO–LUMO Energies for the Reactant Species

	NH_3	NHF_2	CH_3NH_2	CH_2O	CH_3CHO	CF_2O	HOCHO
δ(N)[a]	−0.88	+0.14	−0.79				
δ(NR_2)[b]	−0.30	−0.39	−0.29				
δ(C)[c]				0.13	0.34	1.24	0.63
δ(CR_2)[d]				0.48	0.52	0.53	0.30
LUMO[e]	7.48	6.15	7.46	4.00	4.41	4.22	4.95
HOMO[e]	−10.58	−13.6	−9.88	−11.8	−11.3	−15.0	−12.5

[a] Charge density on the N atom. [b] Charge density on the NR_2 group of NR_2H. [c] Charge density on the C atom. [d] Charge density on the CR_2 group of $CR_2{=}O$. [e] Energy in eV calculated with the 3-21G basis set.

erature.[17] Fully optimized structures and force fields were determined with the 3-21G basis set[18] by using the energy gradient method. The optimized structures were then used for single-point energy calculations with the larger 6-31G* basis set[19] and in some cases at the level of third-order Møller–Plesset (MP3) perturbation theory[20] with the 6-31G* basis set. The calculated transition-state structures and the reaction coordinates are shown in Figure 1. Structural parameters for optimized reactants, transition states, and products are listed in Table I. Tables II and III summarize the activation and the reaction energies for the reactions, charge

---

(17) Oie, T.; Loew, G. H.; Burt, S. K.; Binkley, J. S.; MacElroy, R. D. *J. Am. Chem. Soc.* **1982**, *104*, 6169–6174.

(18) Binkley, J. S.; Pople, J. A.; Hehre, W. J. *J. Am. Chem. Soc.* **1980**, *102*, 939–946.

(19) Hariharan, P. C.; Pople, J. A. *Theor. Chim. Acta* **1973**, *28*, 213–222.

(20) Pople, J. A.; Binkley, J. S.; Seager, R. *Int. J. Quantum Chem. Symp.* **1976**, *10*, 1–19.

Table III. Charge Densities and Activation and Reaction Energies

	1. NH_3–CF_2O		2. CH_3NH_2–CH_2O		3. NH_3–CH_2O		4. NH_3–CH_3CHO		6. NHF_2–CH_2O	
	TS	PD	TS	PD	TS	PD	TS	PD	TS	PD
$\delta(N)^a$	–0.97	–0.93	–0.86	–0.79	–0.91	–0.89	–0.90	–0.84	–0.45	–0.48
$\delta(NR_2)^b$	–0.19	–0.23	–0.18	–0.24	–0.19	–0.24	–0.19	–0.22	+0.67	+0.81
$\delta(C)^c$	1.28	1.34	0.16	0.18	0.16	0.17	0.32	0.31	0.06	0.13
$\delta(CR_2)^d$	0.48	0.54	0.49	0.56	0.50	0.57	0.50	0.54	0.19	0.13
$E_{3\text{-}21G}{}^e$	23.8	–24.9	29.2	–19.7	31.9	–17.8	34.7	–14.4	45.2	–23.5
X^{*f}	0.33		0.37		0.39		0.41		0.40	
$E_{6\text{-}31G^*}{}^e$	41.9	–10.7	42.5	–11.8	45.7	–6.3	49.3	–4.9	61.4	–16.2

[a–d] See footnotes *a–d* in Table II. [e] Activation energy (E_a) for transition states (TS) or reaction energy (ΔE) for products (PD), in kcal/mol. E_a = 40.8 kcal/mol, ΔE = –3.7 kcal/mol, X^* = 0.48 for NH_3–HOCHO at 3-21G (ref 16), E_a = 34.0 kcal/mol, ΔE = –10.6 kcal/mol for NH_3–CH_2O at MP3/6-31G*. [f] Miller's relationship parameter, see eq 2 in text.

Table IV. The Pauling Bond Orders in the Transition States

reactions	$(n_p)_{C\text{-}N}$	$(n_p)_{C\text{-}O}$	$(n_p)_{N\text{-}H}$	$(n_p)_{O\text{-}H}$
1. NH_3–CF_2O	0.58	1.23	0.44	0.28
2. CH_3NH_2–CH_2O	0.60	1.19	0.56	0.23
3. NH_3–CH_2O	0.57	1.28	0.61	0.22
4. NH_3–CH_3CHO	0.55	1.23	0.55	0.23
5. NH_3–HOCHO	0.55	1.23	0.49	0.27
6. NHF_2–CH_2O	0.21	1.38	0.37	0.38

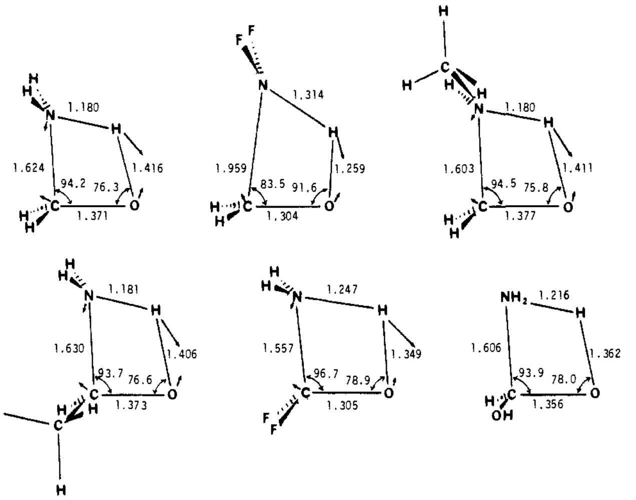

Figure 1. 3-21G transition-state structures. Arrows are the reaction coordinates. The structure of the NH_3–HOCHO system is taken from ref 17.

densities for the compounds at each stationary points, as well as the HOMO and the LUMO energies of the reactant amines and ketones. Cartesian force constants were transformed to the internal force constants using **B** matrices and then the vibrational frequencies were calculated. Isotope effects were determined by Bigeleisen's equation (eq 1) from the calculated frequencies, where u stands for $h\nu/kT$ and $\nu^‡$ is the reaction coordinate frequency.[21] Table V lists the calculated isotope effects. Relaxed force constants, ψ_{ii}, were calculated from the internal force constants as described in the literature.[22] Some of the important relaxed force constants were listed in Table VI.

$$k_1/k_2 = \left[\frac{\nu^‡{}_{L1}}{\nu^‡{}_{L2}}\right] \times \left[\prod_i^{3n^‡-7}\left(\frac{u_{1i}{}^‡}{u_{2i}{}^‡}\,\frac{e^{-u_{1i}{}^‡/2}}{e^{-u_{2i}{}^‡/2}}\,\frac{1-e^{-u_{2i}{}^‡}}{1-e^{-u_{1i}{}^‡}}\right)\prod_i^{3n-6}\left(\frac{u_{2i}}{u_{1i}}\,\frac{e^{-u_{2i}/2}}{e^{-u_{1i}/2}}\,\frac{1-e^{-u_{1i}}}{1-e^{-u_{2i}}}\right)\right] \tag{1}$$

Discussion

Addition of amines to carbonyl compounds was found to occur in a single step through a four-centered transition state in vacuo.

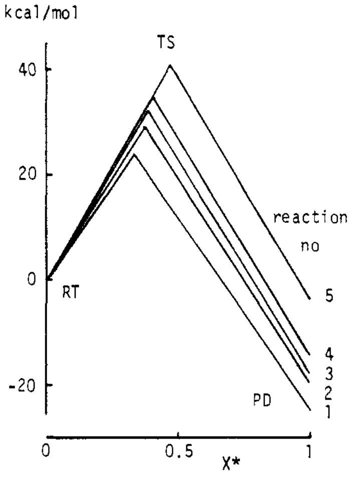

Figure 2. Relations between activation and reaction energies. Abscissa represents X^* values calculated by eq 2 of text.

Similar results have been observed by Williams, Maggiora, Schowen et al. for addition of a water molecule to formaldehyde, in which the zwitterionic intermediate is not a bound species and a concerted addition is an enforced mechanism by the nonexistence of the intermediate along the alternative stepwise route.[23] The four-centered transition states in the present system were found to have C_s symmetry for reactions 1, 3, and 6, while the product amino alcohols have no symmetry in all cases.

Activation and Reaction Energy. All the activation and reaction energies were calculated with both 3-21G and 6-31G* basis sets. The 6-31G* activation energy was found to be uniformly larger than the 3-21G activation energy irrespective of the substituent. Likewise the reaction energy calculated with the 6-31G* basis set is uniformly less negative than that with the 3-21G basis set. Therefore the qualitative trends are the same for the two basis sets. For the discussion below the energy with the 3-21G basis set was used because the same level of calculations are available[16] for a related reaction, NH_3 + HOCHO (reaction 5). Although calculations at this level of theory are known to give only rough estimates for activation and reaction energies,[24,25] we think that qualitative comparison for a series of reactions should be valid. Single-point energy calculations at the MP3/6-31G* level were carried out for the reaction of ammonia with formaldehyde. Both activation and reaction energies were found to lie between those with the 3-21G and 6-31G* basis sets.

As can be seen in Table III, there is a regular relation between the activation and the reaction energy for reactions 1–5; the more exothermic is the reaction, the smaller is the activation energy. Thus, the Bell–Evans–Polanyi–Leffler–Hammond rule[2–4] holds for these reactions. There are a few analytical expressions

---

(21) Bigeleisen, J. *J. Chem. Phys.* **1949**, *17*, 675–678.

(22) Williams, I. H. *Chem. Phys. Lett.* **1982**, *88*, 462–466.

(23) (a) Williams, I. H.; Spangler, D.; Femec, D. A.; Maggiora, G. M.; Schowen, R. L. *J. Am. Chem. Soc.* **1980**, *102*, 6621–6623. (b) Williams, I. H.; Maggiora, G. M.; Schowen, R. L. *Ibid.* **1980**, *102*, 7831–7839.

(24) Rayez-Meaume, M. T.; Dannenberg, J. J.; Whitten, J. L. *J. Am. Chem. Soc.* **1978**, *100*, 747–749.

(25) Pople, J. A. *Ber. Bunsenges. Phys. Chem.* **1982**, *86*, 806–811.

Table V. Kinetic and Equilibrium Isotope Effects[a]

reaction	$^{12}k/^{14}k$ at C=O	$^{16}k/^{18}k$ at C=O	$^{14}k/^{15}k$ at NR_2H	$^{H}k/^{D}k$ at NR_2D
1. NH_3–CF_2O	1.031 (1.002)	1.015 (1.009)	0.966 (0.966)	3.402 (0.946)
2. CH_2NH_2–CH_2O	1.030 (0.985)	1.022 (1.002)	0.976 (0.980)	3.556 (1.036)
3. NH_3–CH_2O	1.035 (0.991)	1.023 (1.010)	0.974 (0.980)	3.485 (0.992)
4. NH_3–CH_3CHO	1.036 (0.985)	1.020 (1.007)	0.970 (0.976)	3.305 (0.933)
6. NHF_2–CH_2O	1.045 (0.979)	1.013 (1.000)	1.005 (0.989)	6.568 (1.498)

[a] Isotope effects at 25 °C. Values in parentheses are equilibrium isotope effects.

Table VI. Relaxed Force Constants and Parameter f for the Addition Reactions of Amines to Carbonyl Compounds[a]

reaction	state	relaxed force constant	
		Ψ_{C-O}	Ψ_{N-C}
1. NH_3–CF_2O	RT	17.06	
	TS	8.14 (0.83)	2.97 (0.52)
	PD	6.30	5.68
2. CH_3NH_2–CH_2O	RT	14.51	
	TS	5.70 (0.93)	2.57 (0.55)
	PD	5.08	4.69
3. NH_3–CH_2O	RT	14.51	
	TS	5.89 (0.88)	2.40 (0.50)
	PD	4.68	4.70
4. NH_3–CH_3CHO	RT	14.39	
	TS	5.98 (0.88)	2.27 (0.53)
	PD	4.83	4.26
6. NHF_2–CH_2O	RT	14.51	
	TS	8.14 (0.72)	0.66 (0.17)
	PD	5.72	3.80

[a] Relaxed force constants are in mdyn/Å. Values in parentheses are f parameters.

presented which relate the position of the activation barrier along the reaction coordinate to the activation and the reaction energy.[5-7] Miller's relationship[6] is the simplest among these relations. Transition-state parameters, X^*, calculated by Miller's relationship (eq 2) are listed in Table III. This expression was used because

$$X^* = \frac{E_a}{2E_a - \Delta E} \qquad (2)$$

of its simplicity, but other equations give the same trend for the series of reactions. Figure 2 shows how nicely the above relation holds.

Reaction 6 deviates from the relation in Figure 2. This is in line with the fact that the transition state for reaction 6 has a structure different considerably from those for reactions 1–5. The difference can be rationalized in terms of the intrinsic barriers of these reactions (vide infra).

Transition-State Structure. Basis set dependence of the calculated structures of ground-state molecules has been examined relatively well and in some cases shown to be large.[26] However, studies on transition-state structures are limited. Recently, Pople reported that in the vinylidene–acetylene rearrangement reaction, refinement of the basis set from HF/3-21G to MP2/6-31G* leads to modest geometrical changes in spite of sharp reduction of the activation barrier.[25] Maggiora et al. also showed that in the addition reaction of a water molecule to formaldehyde, which is a similar reaction to those in the present study, the transition-state structure is not sensitive to the basis set used.[27] These studies indicate that the characteristic features of the transition state of the present reactions are reliable at least qualitatively, although the calculations were carried out with a relatively small basis set (3-21G).

As can be seen in Figure 1, all transition states have similar structures except for the NHF_2–CH_2O case. The similarity for reactions 1–5 is important because the difference in activation energy amounts to 17 kcal/mol (between reactions 1 and 5, corresponding to the rate ratio of about 10^{12}). The situation may more clearly be seen in Table IV, where Pauling bond orders, n_p, for four bonds, N–C, C–O, N–H, and O–H, are shown.[28] The Pauling bond order was given in eq 3, where R is the length of a bond in question in the transition state and R_0 is that in the reactant (for N–H) or in the product (for N–C, C–O, and O–H). The calculated bond orders are nearly the same for reactions 1–5

$$R = R_0 - 0.3 \ln n_p \qquad (3)$$

while they are different for reaction 6. In the former reactions, n_{C-N} is much larger than n_{O-H} and thus the C–N bond formation is far more advanced than the H–O bond formation in the transition state. The situation is reversed for the latter reaction; here n_{O-H} is larger than n_{C-N}.

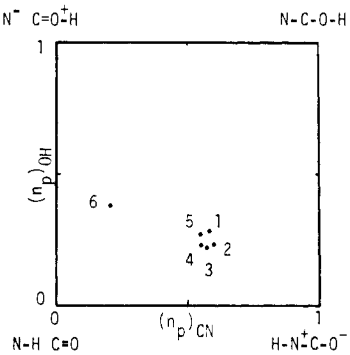

Figure 3. More O'Ferrall–Jencks diagram for the addition reactions.

The present results for reactions 1–5 show that the variation in the position of the activation barrier calculated from energetics does not necessarily reflect the real variation in the transition-state structure. In other words, it is not always correct to draw a conclusion on the variation in the transition-state structure from the variation in reaction rates.

The Marcus theory[7] suggests that the intrinsic barrier, a barrier for a hypothetical thermoneutral reaction, is an important quantity to characterize the reaction. Following the procedure proposed by Murdoch,[29] the intrinsic barriers of reactions 1–6 can be computed as 47.1 (35.1), 50.6 (38.4), 48.8 (40.3), 51.6 (41.6), (42.6), and 69.3 (56.3) kcal/mol, respectively, based on the 6-31G* (3-21G) energies; the intrinsic barrier of reaction 6 is considerably larger than those of reactions 1–5. Accordingly, these reactions are classified into two different families, reactions 1–5 and reaction 6. It is now well recognized that the transition state for a family of reactions varies to a lesser extent if the intrinsic barriers for the reactions are large relative to the change in exothermicity.[30] Clearly the intrinsic barriers of reactions 1–5 are all substantially larger than the exothermicites (–10.7 (–24.9), –11.8 (–19.7), –6.3 (–17.8), –4.9 (–14.4), and (–3.7) kcal/mol, respectively, based on the 6-31G* (3-21G) energies). Thus, the present results are consistent with the theory.

The difference in the transition-state structure between reaction 6 and reactions 1–5 is rationalized in terms of the More O'Ferrall–Jencks diagram[10,11] shown in Figure 3. In this diagram, the lower-left and upper-right corners represent the reactant and the product, respectively, and the upper-left and lower-right corners correspond to the hypothetical structures as shown. The position of the transition state is given by a point. The treatment of the

---

[26] Murdoch, J. R.; Streitwieser, A.; Gabriel, S. *J. Am. Chem. Soc.* **1978**, *100*, 6338–6340.

[27] Spangler, D.; Williams, I. H.; Maggiora, G. M. *J. Comput. Chem.* **1983**, *4*, 524–541.

[28] Pauling, L. *J. Am. Chem. Soc.* **1947**, *69*, 542–553.

[29] Murdoch, J. R. *J. Phys. Chem.* **1983**, *87*, 1571–1579.

[30] Murdoch, J. R. *J. Am. Chem. Soc.* **1972**, *94*, 4410–4418; **1980**, *102*, 71–78.

More O'Ferrall–Jencks diagram predicts that if the upper-left corner is stabilized and the lower-right corner is destabilize by a given perturbation the transition state should shift close to the upper-left corner. The ab initio calculations (3-21G) showed that the difluoro substituents stabilize the negatively charged nitrogen of the amide anion and destablize the positively charged nitrogen of ammonium cation, and thus the shift of the transition state from, for example, 3 to 6 is consistent with the prediction.

HOMO–LUMO Energy Level and Charge Density. Effects of substituents of amines and carbonyl compounds on the activation energy are consistent with the traditional electronic theory. An electron-donating substituent on ammonia decreases the activation energy while that on formaldehyde increases the energy. Population analysis, however, indicated that the electron density on the N atom of amines decreases in the order $H > CH_3 \gg F_2$. Thus, the methyl group is electron withdrawing compared with hydrogen. Similarly the electron density on the carbonyl carbon decreases in the order $H > CH_3 > OH \gg F_2$. It is clear that the reactivities do not follow the order of the electron density.

The frontier molecular orbital energy gap is known to be important in controlling reactivities.[31] This is also true in the present system; the HOMO energy level of the amines goes up in the order $NHF_2 < NH_3 < CH_3NH_2$ (becomes more reactive) and the LUMO energy level of the carbonyl compounds goes up in the order $CH_2O < CH_3CHO < HOCHO$ (becomes less reactive). The exception is CF_2O. Its LUMO energy level is higher than that of CH_2O but it is more reactive than CH_2O. It is conceivable that the reactivity of CF_2O is controlled by the large positive charge density on the carbon atom rather than the frontier molecular orbital energy level.

The change in charge density (excessive negative charge) on the NR_2 moiety on going from the reactant to the transition state is informative. For the reaction of NHF_2 with formaldehyde, the charge density on NR_2 (NF_2 in this case) becomes more negative (−0.39 to −0.45, see Tables II and III), while for the reactions of other amines the charge density becomes less negative; i.e., in the case of NH_3–CH_2O, the charge density on NH_2 varies from −0.30 to −0.19. These variations in charge can be interpreted in terms of the types of the reactions. In case of reaction 6 (NHF_2–CH_2O), the proton transfer is advanced over the C–N bond formation, and therefore the negative charge builds up on the NR_2 moiety in the transition state. On the other hand, for reactions 1–5, the C–N bond formation is more important than the N–H bond breaking. Thus the NR_2 moiety tends to bear the positive charge in the transition state. In other words, the reaction for a less nucleophilic and more acidic NHF_2 is proton transfer in nature while nucleophilic attack to the carbonyl carbon is relatively more important for more nucleophilic and less acidic amines. These conclusions are consistent with the structures of the transition states for these reactions.

Kinetic and Equilibrium Isotope Effects. It has been assumed that the magnitude of a kinetic isotope effect is directly related to a change in force fields which in turn is connected with the structure of the transition state.[14] Hence, kinetic isotope effects are believed to be a good direct measure of the structure of the transition state. The present calculations provide isotope effects, force fields, as well as the structures of the initial and the transition state and therefore an opportunity to test the above assumption.

The apparent and the most important feature of the isotope effects listed in Table V is the similarity in the magnitudes of the kinetic isotope effects for reactions 1–4. These are so similar that it might hardly be possible to distinguish them experimentally if they could be measured. We would find practically the same isotope effects and then conclude that the transition-state structures are the same for these reactions.

As Figure 1 and Table I show, the transition-state structures are indeed similar for these reactions. These results indicate that the structure of the transition state and the kinetic isotope effects are related strongly with each other.

The magnitudes of the kinetic isotope effects for reaction 6 are consistent with its transition-state structure. Large ^{14}C and ^{15}N kinetic isotope effects for reaction 6 compared with those for reactions 1–4 suggest a smaller extent of the C–N bond formation for the former reaction; a smaller ^{18}O isotope effect suggests an advanced O–H bond formation; a large primary deuterium isotope effect for reaction 6 suggests that the hydrogen transfer is the important process of this reaction.[32] It is not possible to draw a semiquantitative picture of the transition state from these isotope effects unless model calculations of these data are carried out, but the ab initio transition-state structure for reaction 6 is certainly consistent with the expectation based on the isotope effects.

Equilibrium isotope effects are similar in all cases except for the primary isotope effect for reaction 6. The similarity is very important because it indicates that the substituents on the stable molecules do not have large influence on the isotopic shifts of the vibrational frequencies. It suggests that any differences in kinetic isotope effects among related reactions can be attributed to differences in the transition state.

It is interesting to see why the equilibrium deuterium isotope effect for reaction 6 is exceptionally large. Since the equilibrium constant for the following isotopic exchange reaction (eq 4) was computed as large as 1.60, it is apparent that the difference in

$$NHF_2 + NH_2D \rightleftharpoons NDF_2 + NH_3 \qquad (4)$$

the equilibrium isotope effect between reactions 1–5 and 6 fully originates in the difference in frequencies between NHF_2 and NH_3. It is noteworthy that the equilibrium isotope effect between NH_3 and NHF_2 observed here parallels that between CH_4 and CHF_3 which can be computed as 1.60 by using Shiner's tabulation of fractionation factor calculations.[33] One might expect that the N–H bond is stronger for NHF_2 than for NH_3, which would give the equilibrium isotope effect of 1.60 for eq 4 because deuterium is known to tend to concentrate in a stronger bond.[33] However, this expectation is not correct; the relaxed force constant (vide infra) for the N–H stretching mode, ψ_{NH}, is 7.44 mdyn/Å for NH_3 and 7.11 mdyn/Å for NHF_2; similarly the N–D stretching vibrational frequency is 2735 cm^{-1} for NH_2D and 2634 cm^{-1} for NDF_2. Thus, the N–H bond is weaker for NHF_2. Vibrational analysis shows that the true origin of the large equilibrium deuterium isotope effect for reaction 6 is a strong isotopic dependence on the bending frequencies of NHF_2. The sum of the decrease in the bending frequencies upon deuterium substitution ($\sum\Delta\nu$) is 669 cm^{-1} for NHF_2 which may be compared with 331 cm^{-1} for NH_3. The importance of bending motions of isotopic hydrogens in determining the magnitude of fractionation factors has been mentioned in the literature.[33]

Force Constants. A relaxed force constant ψ_{ii} is the force to produce a unit displacement in coordinate i while all other coordinates relax to values such that their conjugate internal forces are zero.[22] They can be uniquely defined in contrast to the traditional force constants and thus provides useful information on the extent of structural transformation. Table VI lists the relaxed force constants of selected coordinates. Relaxed force constants for N–H and O–H stretching modes are negative in the transition states and not included in Table VI. Figures in parentheses are the parameter that represents the extent of bonding change in the

---

(31) (a) Fukui, K. *Acc. Chem. Res.* **1971**, *4*, 57–64. (b) Klopman, G. *J. Am. Chem. Soc.* **1968**, *90*, 223–234.

(32) A referee suggested that a proton being transfered between electronegative atoms may lie in a stable potential at the transition state when the proton transfer is coupled with heavy-atom reorganization and that such a proton has a relatively high zero point energy which should be reflected in small hydrogen kinetic isotope effects. Deuterium kinetic isotope effects calculated for the present reactions are large in contrast to this expectation. The proton transfer in the present reactions is an important reaction coordinate mode at the four-centered transition state as shown in Figure 1. This should be the main reason for the difference in the magnitude of the isotope effects between the concerted additions and acid–base catalyzed proton transfer reactions. See: (a) Swain, C. G.; Kuhn, D. K.; Schowen, R. L. *J. Am. Chem. Soc.* **1965**, *87*, 1553–1561. (b) Elison, R.; Kreevoy, M. M. *Ibid.* **1978**, *100*, 7037–7041.

(33) (a) Buddenbaum, W. E.; Shiner, V. J., Jr. In "Isotope Effects on Enzyme-Catalyzed Reactions"; Cleland, W. W., O'Leary, M. H.; Northrop, D. B., Eds.; University Park Press: Baltimore, 1977; Chapter 1. (b) Hartshorn, S. R.; Shiner, V. J., Jr. *J. Am. Chem. Soc.* **1972**, *94*, 9002–9012.

transition state calculated in eq 5. It is apparent that the magnitude of parameter f is similar for reactions 1–4. On the other

$$f = (\psi_{ii}{}^{\ddagger} - \psi_{ii}{}^{\mathrm{react}})/(\psi_{ii}{}^{\mathrm{prod}} - \psi_{ii}{}^{\mathrm{react}}) \tag{5}$$

hand, the values are quite different for reaction 6; in particular the parameter for the N–C bond stretch is very small, which is consistent with the structure of the transition state (see Figure 1). It can be concluded from these results that the force constants are strongly related to the structure of the transition state. It seems reasonable therefore to assume that the magnitudes of kinetic isotope effects are a direct measure of the structure of the transition state.

Comparison with S_N2. Similar investigations have been reported for S_N2 reactions by Wolfe et al.[34] They calculated the structures and the energy of a series of methyl transfer reactions and found that the transition-state structure varies with the change in the reaction energy in a manner expected by the Bell–Evans–Polanyi–Leffler–Hammond rule: the more exothermic the reaction, the more closely the transition-state structure resembles the higher energy reactant. It was also demonstrated by Wolfe[34] and Murdoch[13a] that the Marcus relationship holds for the methyl transfer step between the two ion–molecule complexes of the double-well coordinate. In sharp contrast to the case of S_N2, the present reaction showed that the transition-state structure is essentially unchanged with the change in the reaction energy for reaction 1–5. It emphasizes the importance of the intrinsic barrier in governing substituent effects on the energetics and the geometries of the chemical reactions; the intrinsic barriers of the carbonyl addition reactions are, as described earlier in the Transition State Structure section, substantially larger than the changes in the endothermicity while the intrinsic barriers of S_N2 obtained by Wolfe and Murdoch are in many cases not large compared to the changes in endothermicity.[13a,34] The present study shows that an ab initio MO calculation is useful for increasing our knowledge on the principle of chemical reactions.

Summary

The results of the present study can be summarized as follows. (1) Except for the NHF_2–CH_2O case, the Bell–Evans–Polanyi–Leffler–Hammond rule holds energetically but the structure of the transition state is essentially unchanged. This indicates that the barrier height and the structure of the transition state correlate in different manners with the reaction energy. These results can be rationalized in terms of the magnitude of the intrinsic barrier of the reactions. (2) The differences in the structures of the transition state between the NHF_2–CH_2O case and others is consistent with the prediction based on the More O'Ferrall–Jencks diagram. (3) Both isotope effects and force constants are nicely related to the geometries of the compounds studied. Thus it can be concluded that the kinetic isotope effects are a good measure of the structure of the transition state.

Acknowledgment. Numerical calculations were carried out at the Computer Center of the Institute for Molecular Science.

---

(34) Wolfe, S.; Mitchell, D. J.; Schlegel, H. B. *J. Am. Chem. Soc.* **1981**, *103*, 7692–7694, 7694–7696.

Inductive Effects on the Electron Distribution of the Vinyl Group: A Correlation between Substituent Electronegativity and Bond Point Shift

Tom S. Slee

Contribution from the Department of Chemistry, McMaster University, Hamilton, Ontario, Canada L8S 4M1. *Received May 2, 1985*

Abstract: The complementary merits of two theories are discussed in this paper. One is the perturbational molecular orbital (PMO) theory as applied to σ orbital systems, and the other is a theory of atoms in molecules, and their properties, based on the charge distribution. A case study of a series of substituted ethylenes is reported. It shows how the theory of atoms in molecules provides a useful tool for testing the extent to which PMO predictions concerning substituent effects are realized in good quality wave functions. Conversely it is shown that the PMO model provides a way of estimating—and thus partially understanding—the changes in atomic charges (as uniquely defined by the theory of atoms in molecules) that occur on substitution. Along the way a method of estimating group electronegativities is shown to arise naturally from the PMO treatment of inductive effects.

This paper reports ab initio wave functions at optimized geometries for a series of vinyl compounds and analyzes the electron distributions so obtained. The purpose of these calculations is to test a simple model of substituent inductive effects, namely Dewar's version of perturbational molecular orbital (PMO) theory[1] as applied to σ bonds.

Ab initio calculations provide more direct means for testing models of molecular behavior than experimental data such as equilibrium and rate constants. Thus, they can provide added insight into the accuracy and physical basis of models. The electron distribution is a particularly appropriate tool for the purpose as it enables the predictions of models to be measured against quantities which are well-defined, obtainable directly from experiment in principle, and physically meaningful. One way of obtaining such quantities is to employ a theory of atoms in molecules developed recently,[2] which provides definitions of atoms in molecules based on the topology (the general form) of the electron distribution. The atoms defined by this approach are

---

(1) Dewar, M. J. S.; Dougherty, R. C. "The PMO Theory of Organic Chemistry"; Plenum: New York, 1975.

(2) Bader, R. F. W. *Acc. Chem. Res.* **1985**, *18*, 9–15. Bader, R. F. W.; Anderson, S. G.; Duke, A. J. *J. Am. Chem. Soc.* **1979**, *101*, 1389–1395. Bader, R. F. W.; Nguyen-Dang, T. T.; Tal, Y. *Rep. Prog. Phys.* **1981**, *44*, 894–947.

0002-7863/86/1508-0606$01.50/0